Scaling of Granular Flow Processes: from Surface Flows to Design Rules

J. M. Ottino
Depts. of Chemical and Mechanical Engineering, R. R. McCormick School of Engineering and Applied Science, Northwestern University, Evanston, IL 60208

D. V. Khakhar
Dept. of Chemical Engineering, Indian Institute of Technology - Bombay, Powai, Mumbai 400076, India

Scale-up of granular processes is notoriously difficult and there is little guidance at the present time. This is true even in the simplest case of noncohesive powders consisting of spherical grains, the scenario considered here. However, flows in granular materials are often restricted to thin regions of rapid surface flow with the rest of the material suffering only slow plastic rearrangements. This seemingly trivial observation leads to understanding of the entire system and to the concept that an understanding of surface flows constitutes the key element for scale-up of granular flow processes. A surface flow is characterized primarily by its thickness and the shear rate. For large particles, both are controlled primarily by the Froude number and the particle-size ratio (particle diameter to cylinder radius), whereas material properties have a secondary effect. Modern experimental techniques are yielding further insight into the physics of shear flows and theoretical analysis is providing guidance and scaling insights. The assembly of experimental and theoretical components opens the class of problems dominated by surface flows to serious engineering analysis and predictability. Current understanding is extended and integrated, the governing scaling laws are made explicit, and the results obtained in terms of rules are summarized. The use of the integrated knowledge by means of an example is exemplified.

Introduction

Granular processing is widespread across many industries; examples of systems include rotary kilns, drum mixers, granulators, silos, hoppers and chutes. The current understanding of granular flows is limited. Sources of complications are many, stemming from the interactions between irregularly shaped particles at the microscopic scale and propagating upwards to jamming and the formation of bridges at the mesoscales and nonlinear rheology at the macroscopic scale. Flow-induced segregation of granular mixtures is another source of complexity and often puzzlement.

The analysis of granular systems is difficult compared to fluid flows because the basic governing equations for flow, mixing, and segregation (analogous to the Navier-Stokes and convective diffusion equations) are not yet established. Models to predict segregation in granular flows are rudimentary and applicable only to specific systems. Scale-up is thus very important and often the only avenue for the design of granular flow systems.

Surprisingly, granular materials *present a conceptual advantage with respect to fluids*. Flows of granular materials in many systems of practical interest—particularly tumbling and formation of heaps—are restricted to thin regions of *rapid surface flow*. The weight of the flowing particles is sufficient to achieve close packing densities at depths beyond a few particle diameters from the surface. As a result, flow occurs on a "fixed bed" that deforms plastically with a velocity decaying exponentially with distance into the bed; this motion is typically negligibly small compared to the flow in the shear layer (Komatsu et al., 2001; Jain et al., 2002). The shear layer is the key to understanding segregation. Thus, we arrive at the notion that the understanding of rapid *shear flows constitutes the key building block for the understanding of scale-up of granular flow processes*.

In this article previous studies are unified and extended to analyze what aspects of a granular flow process remain in-

Correspondence concerning this article should be addressed to J. M. Ottino.

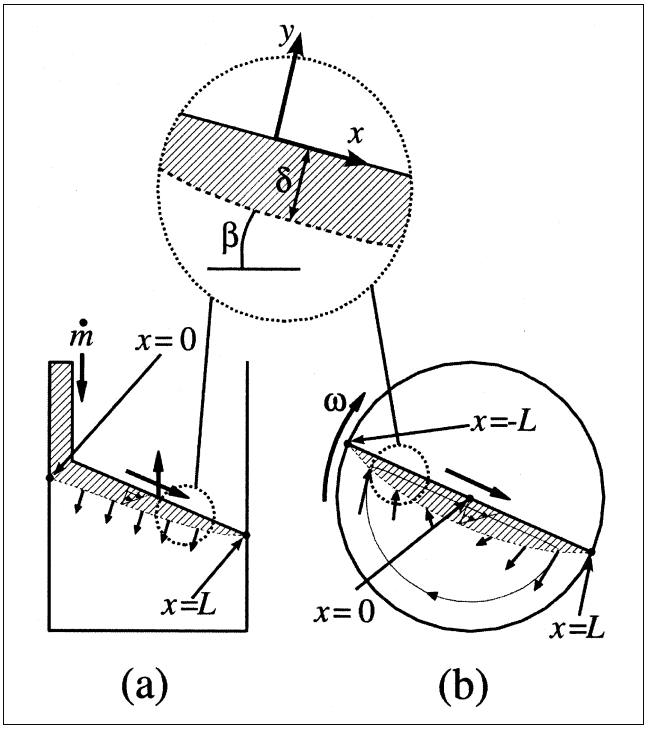

Figure 1. Surface flow systems.

(a) Heap flow; (b) rotating cylinder flow. The coordinate system used in the analysis is shown as an inset.

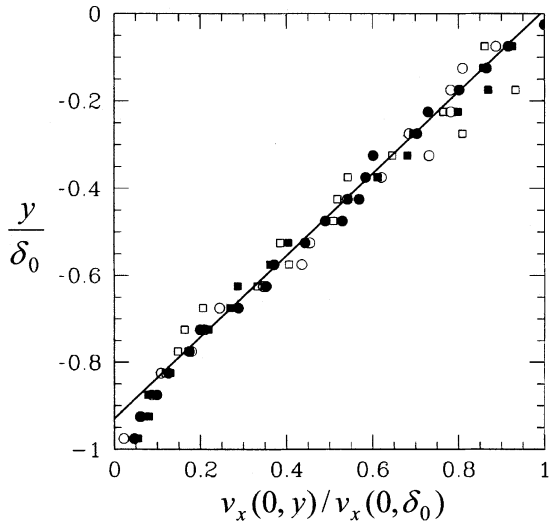

Figure 2. Streamwise velocity profile at $x = 0$ in a rotating cylinder for glass and steel beads normalized with respect to the maximum velocity, v_x $(0, \delta_o)$.

Symbols: ■, glass beads; ●, steel beads. Symbol fill: open, 0.9 rpm; black, 1.6 rpm. The region $0 > y > -0.8$ is well described by a linear profile (Jain et al., 2002).

variant upon change of scale carried out under specified constraints (scale-up rules). This article is organized as follows. First, we describe the rheological parameters and measurements needed to characterize the system. The focus is on surface flows for which most information is available (see Figure 1). Then, we give a summary of results in terms of theory and experiments obtained for two prototypical flows: tumbling in quasi 2-D containers and formation of open and closed heaps. Supporting evidence in the form of experimental plots is presented. The rules extracted provide a setting for the rational design of simple granular processes; they are denoted as **TF** and **HF** for tumbling flows and heaping flows, respectively (Figure 1). An application example is provided at the conclusion.

Rheological Parameters and Measurements

The rheological characterization of granular flow requires the estimation of parameters that depend on the rheological model adopted. For example, the simplest kinetic theory based continuum models typically require the evaluation of the coefficient of restitution, particle diameter (d), and particle density (ρ_p) (Lun et al., 1984). As in the more familiar case of polymeric fluids, phenomenological models have parameters that are not accessible based on a first principles approach, but which must be estimated experimentally. An example belonging to this class is the power law model.

Consider a phenomenological model that allows the calculation of the local shear stress at the bed-layer interface inclined at an angle β with the horizontal. (As we shall see, the interface is not clearly defined; there is a linear region and an exponential decay region of quasi-static motion; the model here simplifies the actual situation; for distances $-\delta < y < 0$, the granular material flows freely, for distances $y < -\delta$ the bed is solid-like.) The shear stress at the interface on the fluid-like side is taken to be

$$\tau_{xy}(-\delta) = c\rho\delta d\dot{\gamma}^2 + \rho g\delta\cos\beta\tan\beta_s \qquad (1)$$

where the first term, quadratic in the shear rate, is the Bagnold collisional stress and the second is the Coulomb friction. The yield stress at the bed-layer interface is taken to be

$$\tau_{xy}(-\delta - d) = \rho g\delta\cos\beta\tan\beta_m. \qquad (2)$$

This model, along with the shape of the velocity profile, gives predictions of surface layer shape, shear rates, and so on, over a wide range of parameters in both tumbling (Khakhar et al., 1997b; Orpe and Khakhar, 2001) and in the formation of heaps (Khakhar et al., 2001a). In the above equations ρ is the bulk density, d is the particle diameter, $\dot{\gamma}$ is the shear rate, and g is the acceleration due to gravity. c, β_s, and β_m are model parameters, and their physical significance is discussed below. The velocity field is assumed linear. This is supported by experimental results (Jain et al., 2001) as shown in Figures 2–3. As noted earlier, the logarithmic region, corresponding to creep flow in the bed, is too slow for being of any consequence to the problems considered here.

We should point out also that for many problems of interest, such as mixing, the precise details of the velocity field in the layer are unimportant; that is, mixing rates and patterns are insensitive to the detail of the velocity field (Khakhar et al., 1999). We note also that, for simplicity, we restrict the discussion here to circular containers. However, the results can be applied to convex containers of any cross sectional shape (such as ellipses, triangles, and squares) and, with suit-

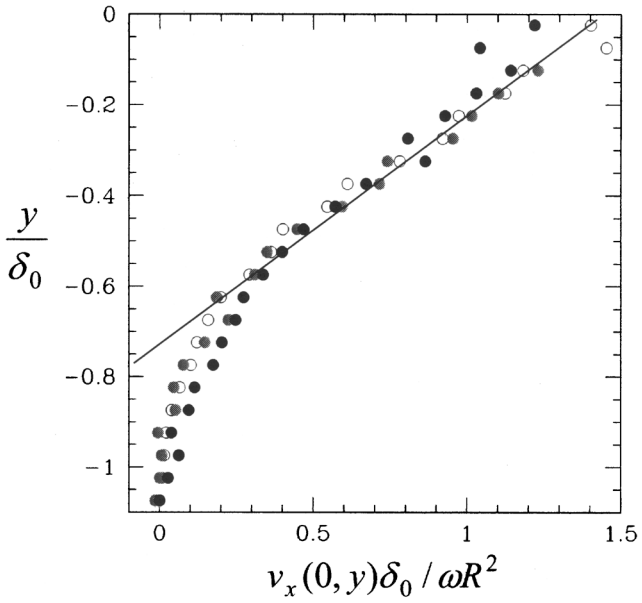

Figure 3. Scaled streamwise velocity profile at $x = 0$ in a rotating cylinder.

(a) 3 mm beads at 0.5, 0.9, and 1.6 rpm; (b) 1, 2, and 3 mm beads at 0.5 rpm. Symbols: ▲, 1 mm beads; ■, 2 mm beads; ●, 3 mm beads. Symbol fill: open, 0.5 rpm; gray, 0.9 rpm; black, 1.6 rpm (from Jain et al., 2002).

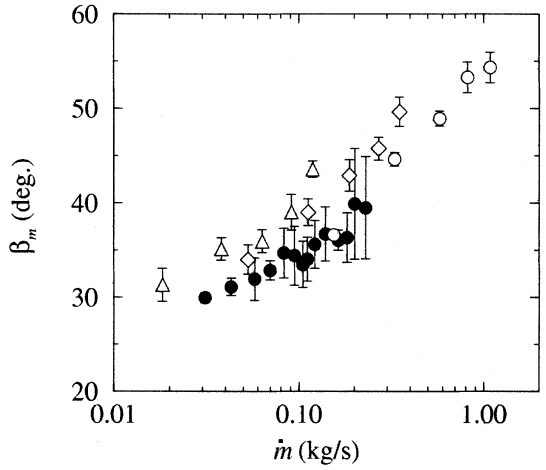

Figure 4. Variation of maximum angle of repose (β_m) with mass-flow rate ($\dot{m}$) for 2 mm steel balls in quasi 2-D systems (depth 10 mm).

Open symbols: rotating cylinder flow; filled symbols: heap flow (Khakhar et al., 2001b).

able modifications, to systems with internal baffles (Hill et al., 1999; Khakhar et al., 1999; Ottino and Shinbrot, 1999).

The phenomenological model for the rheology of surface granular flows, described above, has three parameters:

- c, the dimensionless collisional viscosity;
- β_s, the static angle of repose is the surface angle (with the horizontal) obtained when a steady surface flow is stopped; and
- β_m, the maximum angle of repose (highest permissible angle for steady flow conditions). It is the angle of the bed-layer interface when there is no flux across it, that is, there is no transfer of particles from the flowing layer into the bed and vice versa.

The model parameters can all be evaluated experimentally or calculated in terms of a model.

- The collisional viscosity c can be back-calculated from measurements of the local layer thickness (δ), surface angle (β) and mean velocity (u) (rule **HF6**). For spherical particles, experimental results indicate $c \approx 1.5$, independent of particle size and particle material (Orpe and Khakhar, 2001).
- The static angle of repose β_s can be measured by means of heap formation or tumbling. This is the angle formed after rotation is stopped in tumbling or after mass-flow rate is stopped in the formation of a heap. Both give roughly similar values for a given material, however, a systematic study of this issue is not available.
- The maximum angle of repose β_m can be measured as the free surface angle in steady open heap experiments (flow in the system of Figure 1a with the far wall removed) or the angle at the midpoint of the free surface in tumbling experiments. In both cases the condition of no flow between the bed and layer is satisfied. The data can be correlated with the local flow rate, and both systems give similar results (an example of which is shown in Figure 4 for the case of steel balls).

Current Knowledge

The knowledge of the dynamics of granular surface flows has progressed substantially in the last two years. Here, we unify and extend results presented in the following works: Komatsu et al. (2001) [experimental study of flowing layer, focusing on creep region], Orpe and Khakhar (2001) [properties of flowing layer, mostly experimental], Jain et al. (2001) [experimental particle image velocimetry (PIV) study of flow in layer], Khakhar et al. (2001a) [experimental and theoretical study of surface flow in heap formation], and Khakhar et al. (2002) [theoretical comparison of surface flows occurring in heap formation and tumbling]. It will be apparent that the integration of the knowledge obtained can be translated into predictive equations and relations (with coefficients that can be obtained by means of experiments). This leads to a combination of building blocks that can be assembled for design and scale-up purposes.

Knowledge based on studies of rotating cylinder flow (tumbling flow, TF)

The three primary dimensionless parameters characterizing granular flow in a partially filled cylinder are the Froude number $Fr = \omega^2 R/g$, where ω is the rotational speed of the cylinder and R is the cylinder radius or some suitable length scale, the size ratio $s = d/R$, and the fraction of the cylinder cross-section filled with particles f. Keeping other parameters fixed, increasing the rotational speed causes several flow regime transitions: avalanching to rolling to cascading to cataracting and finally centrifuging. *A priori* prediction of the regime of flow given the system parameters is currently not possible. Henein et al. (1983), however, have shown that the transition from avalanching to rolling depends on Fr and s. Results for the transverse flow are available primarily for the rolling and cascading regimes, and these results are listed below.

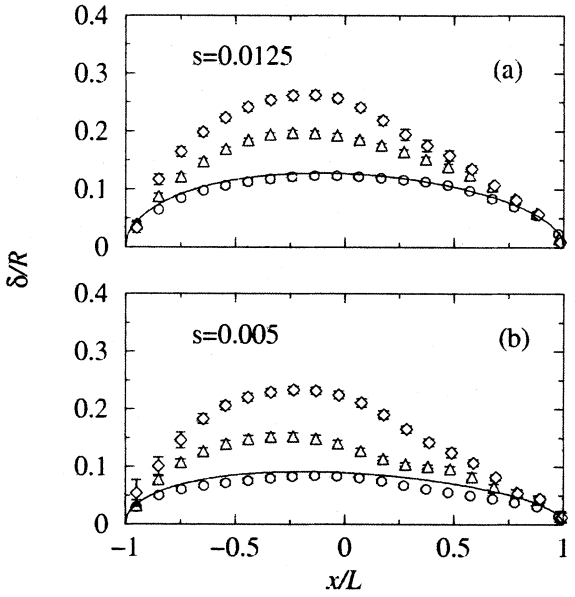

Figure 5. Layer thickness profiles in a rotating cylinder for (a) 2 mm steel balls and (b) 0.8 mm sand.

Symbols denote experimental data for three different Froude numbers (Fr): ○ −0.002, △ −0.022, ◇ −0.064. Solid lines are predictions of the theory (Khakhar et al., 2001b).

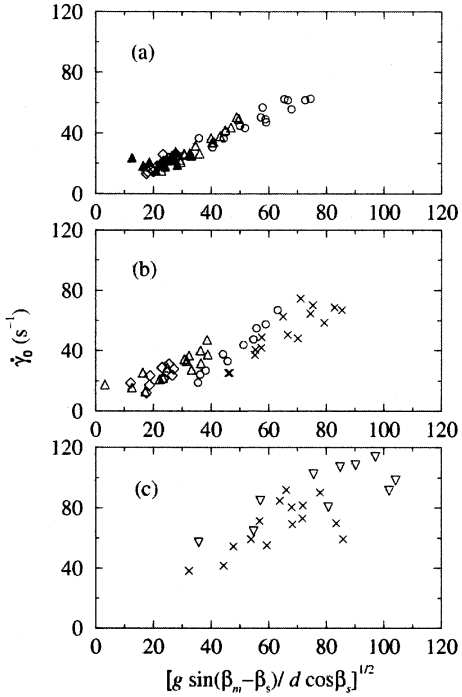

Figure 6. Variation of the computed shear rate at the midpoint ($\dot{\gamma}_0$) for different size ratios and Froude numbers vs. the characteristic shear rate $[g \sin(\beta_m - \beta_s)/d \cos \beta_s]^{1/2}$ for various particles at different rotational speeds and different cylinder sizes.

(a) Steel balls; (b) glass beads; (c) sand particles. Open symbols: data from tumbling experiments; filled symbols: data from open heap system (Khakhar et al., 2001). Note that the slope is approximately the same in all systems.

TF1. PIV experiments show that the velocity profile throughout most of the layer $v_x(y)$ is linear and scales as $v_x/v_{x,\max} = F(y/\delta)$ and the scaling is independent of particle size (Jain et al., 2001). See Figure 2.

TF2. PIV experiments show that the velocity in plastic deformation bed is logarithmic (Komatsu et al., 2001; Jain et al., 2001). See sections in Figures 2 and 3 near $y/\delta_0 = -1$.

TF3. PIV experiments show that the velocity v_x corresponding to several particle diameters can be collapsed (Jain et al., 2001) when plotted as $v_x \delta_0/(\omega R^2)$. See Figure 3.

TF4. PIV experiments show that the velocity v_x corresponding to several rotational speeds can be collapsed (Jain et al., 2001) when plotted as $v_x \delta_0/(\omega R^2)$.

TF5. The volumetric flux per unit width in the flowing layer is maximum at the midpoint and is given by $Q = \omega(R^2 - x^2)/2$ (Rajchenbach, 1990; Khakhar et al., 1997b, 2001b).

TF6. The layer thickness profile of the flowing surface layer is symmetric at low Fr and is given by $\delta = (\omega/\dot{\gamma})^{1/2}(R^2 - x^2)^{1/2}$ for a half-full cylinder (see Figure 5) and the shear rate is nearly constant along the layer (Makse, 1999; Khakhar et al., 2001b). At higher Fr and smaller s, the profiles become skewed (see Figure 5) and the shear rate varies along the layer (Orpe and Khakhar, 2001). The layer shape depends on the particle shape as well. For example, cubical particles (salt) gave an asymmetrical profile (Khakhar et al., 1997b).

TF7. The shear rate at the midpoint of the layer, corresponding to thickness δ_0, is given by $\dot{\gamma}_0 = [g \sin(\beta_m - \beta_s)/cd \cos \beta_s]^{1/2}$ for all Fr and s (Orpe and Khakhar, 2001). See Figure 6.

TF8. The thickness of the layer at the midpoint is given by $\delta_0/R = (\omega/\dot{\gamma}_0)^{1/2}$ for all Fr and s, with $\dot{\gamma}_0$ given by the above expression. Thus, $\delta_0/R \propto (\omega^2 d/g)^{1/4}$ (Makse, 1999; Khakhar et al., 2001b).

TF9. Flow in the layer depends primarily on Fr and s, and material properties, such as restitution coefficients, have a secondary effect. Layer shape profiles for different materials (glass beads, steel balls, and sand) and cylinders of different sizes can be scaled keeping Fr and s fixed (Orpe and Khakhar, 2001). See Figure 7.

TF10. In the case of noncircular cylinders the layer thickness (δ) and layer length (R) vary with time (t), but their ratio $\delta(t)/R(t)$ is constant (Khakhar et al., 1999; Ottino and Khakhar, 2000).

TF11. In the limit $s \to 0$, the collisional term becomes negligible and the flow is purely frictional (an analytical result for this case is given in Rao et al. (1991)). As a consequence, the particles accelerate throughout, the mean velocity increases with distance along the layer, and the layer thickness profile is skewed. The parameter c is not required in the calculations in this limit.

TF12. The flux of particles from the layer into fixed bed (Γ) depends on the difference between the local interface angle (β) and the maximum angle of repose (β_m) with $\Gamma = V(\beta_m - \beta)$ and with $V = g/\dot{\gamma} \cos \beta_m$. Thus, material goes from the layer into the bed when the local angle is less than the maximum angle of repose and vice versa.

TF13. The dimensionless maximum velocity of particles at the free surface of the flowing layer $\bar{u}_m = (u_m/e\omega L \sin \beta)(d/2R)^{1/2}$ is in the range (06,0.8) for $Fr \in (0.004, 0.016)$,

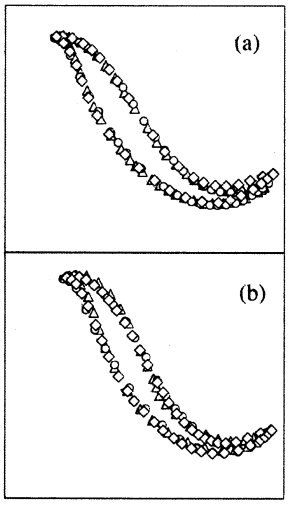

Figure 7. Layer shape profiles for different materials in cylinders of different sizes for Froude number Fr = 0.064.

(a) Steel balls and glass beads with $s = 0.0125$: ○ steel balls with $R = 16$, △ steel balls with $R = 8$, ◇ glass beads with $R = 16$ cm. (b) Sand and glass beads with $s = 0.005$: ○ sand with $R = 16$ cm, △ sand with $R = 8$, ◇ glass beads with $R = 16$ cm (Orpe and Khakhar, 2001).

where e is the coefficient of restitution of the particles (Ding et al., 2001).

A few rules pertain to mixing and segregation in the rotating cylinder. These are listed below.

TF14. Experimental studies of mixing of identical but different colored particles in a rotating cylinder (Khakhar et al., 1997b) and scaling analyses (Savage, 1993) indicate that the collisional diffusivity of particles in the flowing layer may be estimated by $D_{\text{coll}} = 0.025 d^2 \dot{\gamma}$.

TF15. The rate of mixing increases monotonically with decreasing fill fraction. However, when normalized with the mass of material being mixed, the mixing rate is highest for a fill fraction of about 25% (Khakhar et al., 1997b).

TF16. The *axial* dispersion coefficient in a rotating cylinder may be estimated in terms of the diffusivity as $D_a = D_{\text{coll}} t_l / t_b$, where t_b is the average time spent by particles for a single pass through the bed and t_l is the average time spent by particles for a single pass through the layer (Rao et al., 1991).

TF17. The segregation flux of the lighter particles (opposing ordinary diffusion) in a mixture of equal sized but different density particles flowing in a surface layer is given by $J_L = 2C_s(1-\bar{\rho}) D_{\text{coll}} n(1-n)/d$, where n is the number fraction, $\bar{\rho} \le 1$ is the ratio of particle densities, and $C_s \approx 2$ is a model parameter (Khakhar et al., 1997a).

TF18. The optimal rpm which gives best mixing in tumbling mixers scales as $N_{\text{opt}} = C(d/R)$ with $C = 121$ (Fan et al., 1990).

Knowledge based on studies of heap formation (heap flow, HF)

The flow on the surface of a heap shares many similarities with the surface flow in a rotating cylinder. We list some of the common features below.

HF1. In both systems, when the flows are relatively slow, the layer thickness is given by $\delta \propto (Q/g)^{1/2}$, where Q is flux of particles in the flowing layer (Khakhar et al., 2001b).

HF2. As in tumblers, the thickness of the layer in closed heap systems varies as $\delta \propto (L-x)^{1/2}$, where x is the distance from the pouring point and L is the length of the layer.

HF3. In both systems the maximum angle of repose correlates with the flow rate $\beta_m(Q)$ and the measured values are nearly the same for heap flow and rotating cylinder flow (Khakhar et al., 2001b) as mentioned above.

HF4. As in tumblers, the flux of particles from layer to the heap is given by the same expression (Khakhar et al., 2001b).

HF5. When the flow is slow, the shear rate in a heap flow scales in the same way as given in TF7 for the rotating cylinder flow.

The knowledge contained in the above rules allows for a rational analysis of systems of engineering interest. Consider an illustrative example. The example considers the spray

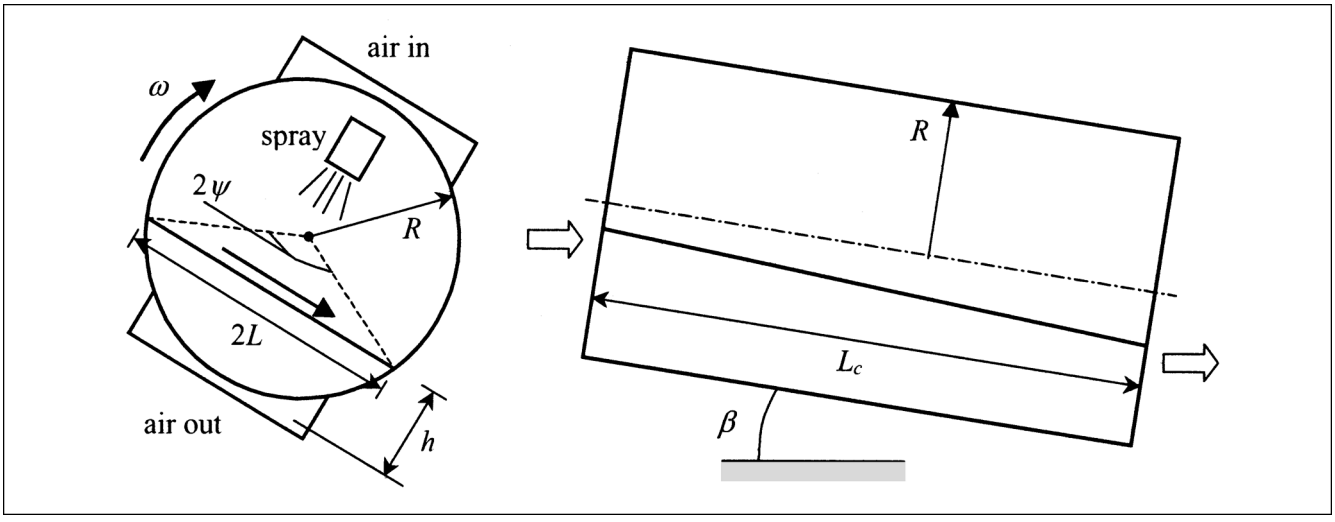

Figure 8. Spray coating system.

Left: View of cross-section; right: view of longitudinal section of continuous coating system. The system parameters are defined.

coating of spherical beads of diameter d placed in a rotating cylinder of radius R and length L_c with a superposed axial flow. We will consider decomposing the system operating in two different modes. First, we consider the batch case (no axial flow) and then the continuous case (with axial flow). It will become apparent that the solution to the problem presented hinges critically on the estimation of the shear rate and the thickness of the layer (rules **TF5-TF8**), and the diffusive mixing (rules **TF13** and **TF14**). As we shall see, all other aspects can be assembled using standard chemical engineering tools.

Example Problem: Analysis of Spray Coating

The cross-section of the system is shown in Figure 8. A uniform spray of a coating solution is applied on the free surface of the flowing particles. A continuous stream of air is blown through the perforated drum as shown to evaporate the solvent and deposit a coating on the beads. The objective is to deposit a coating of a uniform, specified thickness on the beads; initially, the diameter of the beads is d, and the coating thickness at the end of the coating process is d_c. We analyze the rate of mixing and rate of coat deposition based on the models discussed in the previous section.

We assume that the rotational speed of the cylinder is in the rolling/cascading regime to ensure reasonable cross-sectional mixing ($Fr \in (0.002, 0.064)$ for $s \in (0.005, 0.05)$, based on the scaling results). Although mixing in the avalanching regime is faster on a per rotation basis, as mentioned earlier, rolling is faster on a "time" basis, since the rotation rate is so much higher. Further, the spray rate is assumed to be slow enough so as not to wet the flowing layer to such an extent as to prevent it from flowing freely; this is the most critical assumption. Wetting leads to cohesion and this may significantly affect the behavior of small particles (Nase et al., 2001). In practice the rate would depend on both the rate of cross-sectional mixing and the rate of evaporation of the solvent. Other complications may arise, of which the most important is that differences in particle properties may lead to segregation; this issue is not considered here. We will assume that we have measured in the laboratory the rheological parameters β_m, β_s, and c, and that the correlations for the layer thickness, shear rate, diffusivity and axial dispersion are valid (**TF6-TF8, TF13** and **TF15**).

Batch coating

Consider a fixed mass of beads in a cylinder of radius R and length L_c such that the fill fraction is f. Note that we must have $f < 0.5$ since $f > 0.5$ results in an unmixed core that remains completely uncoated (see final section).

For the spray system, the important parameters are the solute concentration and the rate of spraying. These two parameters together determine the batch time for coating, assuming that all the sprayed material is deposited on the particles.

It is also reasonable to assume that, due to the relatively high bulk densities in the rolling/cascading regime, only the top layer of the flowing particles receive the spray. Further, we assume that the spray rate is small relative to the rate of cross-sectional mixing (inverse of the mixing time for complete cross-sectional mixing) to ensure that every particle appears at the free surface several times and, hence, the coating is statistically uniform. We estimate below the time for complete cross-sectional mixing (t_{mix}) and the required batch time of operation (t_{batch}) to achieve the design objectives. The design condition is, therefore, $t_{\text{batch}} \gg t_{\text{mix}}$.

In the rotating cylinder flow, mixing occurs only in the flowing layer since there is no relative motion between particles in the fixed bed. Further, since the flow is steady, the streamlines are time-invariant (Hill et al., 1999) and mixing occurs only as a result of collisional diffusion transverse to the streamlines in the layer. Denote by t_l, the average residence time of particles for a single pass through the layer. An estimate of the diffusional distance traveled by a particle normal to the streamline in a single pass through the flowing layer is then

$$\Delta y \sim \sqrt{D t_l} \tag{3}$$

We take the criterion for complete mixing to be $N_{\text{mix}} \Delta y \sim \delta_0$ where N_{mix} is the necessary number of passes through the flowing layer so that the particles diffuse the equivalent of the maximum layer thickness for complete mixing. Therefore, the number of passes through the flowing layer for complete mixing is

$$N_{\text{mix}} \sim \frac{\delta_0}{\sqrt{D t_l}}. \tag{4}$$

The time for mixing is then the product of the number of passes times the time per pass

$$t_{\text{mix}} = \frac{A \delta_0}{\sqrt{D\tau}} \left(t_l + \frac{2\psi}{\omega} \right) \tag{5}$$

The term in the parentheses is the average time for a pass. It is the sum of the residence time in the layer t_l, and the circulation time in the bed, which can be obtained as $2\psi/\omega$, where 2ψ is the angle subtended by the free surface at the cylinder axis (see Figure 8). The coefficient A can be obtained by fitting experimental data for mixing of identical, but different, colored particles as shown below.

The mean residence time in the layer is $t_l = \int_L^L dx/u$, where $2L$ is the length of the free surface. The mean velocity in the layer is $u = \dot{\gamma}\delta/2$. Using **TF6** (valid for low Fr flow), we obtain

$$t_l = 2\int_0^L \frac{dx}{u} = \frac{4}{(\omega\dot{\gamma}_0)^{1/2}} \int_0^L \frac{dx}{(L^2 - x^2)^{1/2}} = \frac{2\pi}{(\omega\dot{\gamma}_0)^{1/2}} \tag{6}$$

where the shear rate is given by **TF8**.

The time for mixing is then given by

$$t_{\text{mix}} = \frac{A}{\omega} \left(\frac{\pi \delta_0 Pe}{2L} \right)^{1/2} \left[\frac{\delta_0}{L} + \frac{4\psi}{\pi} \right] \tag{7}$$

where $Pe = \omega L^2/D_{\text{coll}}$ is the Péclet number for transverse mixing where D_{coll} is given by **TF14**. From the geometry of the system, we have $L = [R^2 - (R-h)^2]^{1/2}$ and $\psi = \sin^{-1}$

Table 1. Mixing Time in a Rotating Cylinder *

δ_0/L	h/R	L/R	ψ (Deg)	Pe	$(\omega t_{mix}/2\pi)_{exp}$ (Rev.)	$(\omega t_{mix}/2\pi)_{th}$ (Rev.)
0.10	1.00	1.00	90	104	57	57
0.10	0.78	0.97	77	104	19	49
0.10	0.65	0.94	69	104	16	44
0.13	0.75	0.97	75	3×10^3	11	10
0.13	0.58	0.91	65	3×10^3	7	8

*Comparison of predictions of model with estimates from experimental results of Khakhar et al. (1997b) for different systems. Value of fitting parameter used is $A = 4.33$.

(L/R) (see Figure 8 for definition of h). The mixing time computed using these results, denoted t_{mix}, and expressed as cylinder revolutions $(\omega t_{mix}/2\pi)$, is compared in Table 1 to the estimates from the experimental results of Khakhar et al. (1997), denoted *exp*, for different systems for a fitted value of the parameter $A = 4.33$. The model presented above gives a reasonable estimate of the mixing time.

The batch time for coating is determined by a mass balance as the time to deposit a coating of thickness d_c on each particle, assuming that each particle is uniformly coated. Suppose that the total mass of beads in the bed is m, and their density is ρ_p. An estimate of the number of particles in the bed is then $6m/\pi d^3\rho_p$. If the thickness of the coating d_c is such that $d_c \ll d$, then the mass of solute coating each particle is $\pi d^2 d_c \rho_s$, where ρ_s is the density of the coating, and, therefore, the *total* amount of solute to be deposited is $6m\rho_s d_c/\rho_p d$. This corresponds to a volume of the coating solution given by $6m\rho_s d_c/\rho_p d C_s$, where C_s is the concentration of the solute in the solution. Therefore, the batch time for coating is given by

$$t_{batch} = \frac{6m}{QC_s}\frac{\rho_s d_c}{\rho_p d}, \tag{8}$$

where Q is the volumetric spray rate of the solution. The mass of the batch m is related to the fill fraction by $m = \pi R^2 L_c f \rho_b$, where ρ_b is the bulk density.

The condition for obtaining a uniform coating is then $t_{batch}/t_{mix} \gg 1$, which on substitution of the results for the batch and mixing times gives

$$\frac{6m}{AQC_s}\frac{\rho_s d_c}{\rho_p d}\left(\frac{2L}{\pi Pe\,\delta_0}\right)^{1/2}\left(\frac{\delta_0}{L}+\frac{4\psi}{\pi}\right)^{-1} \gg 1. \tag{9}$$

In the above equation, the midlayer thickness δ_0 is given by **TF8** as $\delta_0/L = (\omega/\dot\gamma_0)^{1/2}$, and by **TF7**, the shear rate can be estimated as $\dot\gamma_0 = [g \sin(\beta_m - \beta_s)/cd \cos\beta_s]^{1/2}$. Using **TF13**, the Péclet number is given by $Pe = 40\omega^2 L/d\dot\gamma_0^2$. The parameters ψ, m and L depend on the fill fraction f, which is related to the depth of the bed by $f = [\tan^{-1}(R/h-1) - h/L]/\pi$. From **TF15**, the recommended fill fraction is 25%. Thus, the design parameters to achieve the desired coating should be chosen so that condition 9 is satisfied.

Continuous coating

Consider the extension of the ideas to the continuous coating case. The analysis is similar to that for the batch case. In this case beads are continuously fed to the cylinder at one end and the coated beads flow out of the other end (Figure 8). A uniform spray of the coating solution is applied on the surface of the flowing particles as they move through the cylinder. Similarly to the previous case, the mean residence time t_{res}, required for the particles in the cylinder to achieve a coating thickness t, is then

$$t_{res} = \frac{6m}{QC_s}\frac{\rho_s d_c}{\rho_p d}, \tag{10}$$

where m is the mass holdup of beads in the cylinder. And again, for uniform coating, we must have $t_{res}/t_{mix} \gg 1$ which simplifies to Eq. 9.

An additional factor that is important in the case of a continuous system, but not for batch systems, is axial dispersion. Axial dispersion in the continuously operated coater results in a distribution of residence times, and, thus, in a distribution of coating thicknesses. Since the rate of spraying is constant, the coating thickness is proportional to the residence time. An estimate of the standard deviation of the coating thickness (σ) from the mean value (d_c) is

$$\frac{\sigma}{d_c} = \frac{\sqrt{D_a t_{res}}}{L_c} \tag{11}$$

where D_a is the axial dispersion coefficient. It is apparent that good cross-sectional mixing requires high residence times, that is, lots of cross-sectional turnover times before particles exit the system. This is necessary to have all particles being exposed to the spray. It should be recognized, however, that this produces greater axial dispersion and, thus, a greater standard deviation in the coating thickness. For uniform coating, we thus require long cylinders so that the variation in coating thickness (due to varying residence time in the cylinder) is minimized (Eq. 11).

Conclusions and Open Questions

The central point of this article is that an interpretation, extension, and integration of available understanding of granular flows emanating from fundamental theory, experiments, and simulations is ripe for exploitation in engineering design applications. This understanding can be summarized in terms of scaling laws.

This approach, unaided, is clearly insufficient. A successful design may require the confluence of many viewpoints. Let us briefly consider the roles of direct simulation and experiments and make a few comments about their uses and possible limitations. Consider first the case of theory and direct simulations. It is illustrative to contrast the cases of fluids and solids. For fluids mixing, *basic* understanding at a *continuum level* is firmly established: Navier-Stokes equations provide a first principles description valid on macroscopic scales for most problems. Such an understanding is lacking in the case of granular materials. A change in the nature of a fluid

is reflected in the nature of the constitutive equation—for example, going to a Maxwell model or any type of viscoelastic model. A problem can thus be easily formulated, although perhaps not easily solved (even numerically). No such route is possible in the case of granular materials. Constitutive equations have not been successfully developed—certainly not to the level encountered in fluids. In some restricted contexts, it may indeed be possible to generate flow and constitutive equations. It is in general unclear which material properties may be generic, which are specific to a problem, and when very minor changes in particle properties have large effects. And all of this does not consider the effects of segregation.

The alternative to theory is simulation. Particle dynamics (PD) come close to the ideal of a first-principles approach. The technique is based on the methodology of molecular dynamics developed for the study of liquids and gases. In the simplest case, when the grains are large (say 100 μm or more), the interactions are purely mechanical. The motion of the particles is governed by Newton's laws; the goal of PD simulations is to compute the evolution of linear and angular momentum of every particle by using appropriate contact force models. In principle, "exact" PD simulations require precise physical properties (Young modulus, restitution coefficients, Poisson ratios, and so on). Predictive calculations for specific materials with complex shapes and multidispersed shapes are, in general, nearly impossible. The number of particles is limited to about $10^4 - 10^5$ (Cleary et al., 1998) in contrast to practical systems which have $\gg 10^9$ particles. It would be unwise to recommend PD as the sole source of design guidance. Results depend on the contact force model used (and, by no means, is there a single unequivocal choice). Thorough studies of the parametric sensitivity of the results to model parameters are very much needed.

Consider now the role of *experiments*. Carefully designed experiments are invaluable. The drawback is that results are specific, and it is time-consuming to explore large regions of parameter space. However, a carefully designed experiment can answer questions that would be hard, if not impossible, to answer by other means.

There are two kinds of experiments: qualitative flow visualization techniques and experiments involving measurements. Both classes of experiments serve different roles.

Consider *measurements*. Significant advances have occurred in the last 4–5 years. For example, it is now possible to investigate the interior of granular materials via magnetic resonance imaging (MRI). This technique, however, is years away from becoming a routine industrial practice, and cost is an issue, as well as the kinds of flows that can be examined (the apparatus has to fit within the MRI machine). Finally, the MRI technique places restrictions on the kinds of particles that can be used. Another promising technique is the Positron Emission technique. These two techniques can be used to measure the velocity field in opaque materials (as most of the granular materials are). However, relatively simple techniques can provide valuable insight. For example, many of the results, summarized in the current knowledge section—velocity fields, layers thicknesses—are based on particle image velocimetry (PIV) and particle tracking velocimetry (PTV). The restriction of these techniques is that measurements are restricted to 2-D flows. However, 2-D experiments are relatively easy to implement. In fact, for diagnostic purposes, simple photographic experiments may suffice.

2-D experiments are fast, inexpensive, and reproducible. They can be conducted using a variety of particles. A few precautions must the taken. When the particle size is less than 1 mm in diameter, effects, such as clumping due to moisture or attractive and repulsive forces due to static electricity, are typically important. Also, when the particles are about 0.1 μm or less, cohesive effects are significant. Thus, it is recommended that beads sizes not smaller than 0.5 mm in diameter be used. To minimize axial segregation effects, it is recommended that the depth of the tumblers used be limited to a few particles, say 5–10. The design of the mixers is simple. The faceplate of the mixers can be made of Plexiglas for ease in observation, while the rear plate may be fashioned of aluminum and can be grounded to minimize electrostatic effects.

Several types of experiments are possible. Flow patterns, seeding an initial region, divide the mixer into two large sections. Flow patterns may be obtained with long exposure photographs; seeding experiments rely on identifying a small region and observing it as it deforms in time. Dividing the mixer into large sections, say half of the container with one color and the other half with another color, is relatively easy to implement and allows for observation of evolution of mixing, for example. Segregation experiments are easiest. The initial condition corresponds to a well-mixed system.

Many such experiments have been conducted over the past 5–7 years. What follows is series of design recommendations. (A good reference for this is McCarthy et al. (1996) and Ottino and Shinbrot (1999)).

Whenever possible seek guidance from quasi 2D experiments. This is the easiest way to assess effects such as degree of filling or the effect of baffle geometry or any other geometrical changes. Mixing times can easily be estimated in these systems using tracer experiments.

One typical use is to understand the effects of nonmixing regions or cores. By including baffles, we can deliberately cause avalanches to penetrate the core, and thereby involve it in mixing. McCarthy et al. (1996) show a sequence of sketches depicting what occurs as a tumbler with protruding baffles is slowly rotated.

Be prepared for surprises. Sometimes one baffle is better than two (see McCarthy et al. (1996)): A system with only one protruding baffle as shown works, but a mixer with two baffles placed on opposite sides of the drum *does not* produce better results than one without baffles. Another somewhat unexpected result has to do with 2-D systems that are rotationally asymmetric such as a bent star. Clockwise rotation and counter-clockwise rotation may behave very differently: one will leave an unmixed core, the other will not. These effects have been confirmed experimentally.

The degree of filling is critical. With everything being fixed, the geometry of mixers and materials, the degree of filling is often the only remaining control parameter. The effects of the degree of filling—especially in cases with segregating materials—is of utmost importance.

Simple scaling rules often suffice. In spite of the complexity of granular flows, at macroscopic scales, simple scaling rules can give a good description of system behavior and these are in some cases nearly independent of material type.

A few general remarks about design of granular processes in general—and not just surface dominated flows—may be appropriate at this point. The main lesson that should be extracted from the present work is that, as advocated in Ottino and Khakhar (2001), there is sufficient fundamental knowledge that when filtered and aggregated it can be organized into a coherent whole that leads to practical applications. The case considered here is surface-dominated flows, but the same program—possibly not now, but at some point in the near future—should be carried out for convection and vibration (for a general overview see Duran (2000)) and flows induced by motion of blades (Laurent et al., 2000; Laurent and Bridgwater, 2002; Stewart et al., 2001). It is also clear that the example presented here—owing to spraying—could in the future be sharpened with recent and ongoing work in the area of wet systems (Albert et al., 1997; Nase et al., 2001; Samadani and Kudrolli, 2000). Eventually, one can imagine that the case of slurries (Jain et al., 2001) should be amenable to similar analysis.

Acknowledgment

This work was supported by the Division of the Office of Basic Energy Sciences of the Department of Energy. DVK acknowledges the support from DST, India via the Swarnajayanti Fellowship project.

Literature Cited

Albert, R., I. Albert, D. Hornbaker, P. Schiffer, and A.-L. Barabási, "The Angle of Repose in Wet and Dry Granular Media," *Phys. Rev. E*, **56**, R6271 (1997).

Cleary, P. W., G. Metcalfe, and K. Liffman, "How Well Do Discrete Element Granular Flow Models Capture the Essentials of Mixing Processes?" *Appl. Mathematical Modeling*, **22**, 995 (1998).

Ding, Y. L., R. N. Forster, J. P. K. Seville, and D. J. Parker, "Scaling Relationships for Rotating Drums," *Chem. Eng. Sci.*, **56**, 3737 (2001).

Duran, J., *Sands, Powders and Grains. An Introduction to the Physics of Granular Materials*, Springer-Verlag, New York (2000).

Fan, L. T., Y.-M. Chen, and F. S. Lai, "Recent Developments in Solids Mixing," *Powder Technol.*, **61**, 255 (1990).

Henein, H., J. K. Brimacomble, and A. P. Watkinson, "Experimental Study of Transverse Bed Motion in Rotary Kilns," *Metall. Trans. B*, **14B**, 191 (1983).

Hill, K. M., D. V. Khakhar, J. F. Gilchrist, J. J. McCarthy, and J. M. Ottino, "Segregation-Driven Organization in Chaotic Granular Flows," *Proc. of National Acad. of Sciences*, **96**(21), 11701 (1999).

Jain, N., D. V. Khakhar, R. M. Lueptow, and J. M. Ottino, "Self-Organization in Slurries," *Phys. Rev. Letters*, **86**(17), 3771 (2001).

Jain, N., J. M. Ottino, and R. M. Lueptow, "An Experimental Study of the Flowing Granular Layer in a Rotating Cylinder," *Phys. Fluids*, **14**, 572 (2002).

Khakhar, D. V., A. V. Orpe, P. Andresén, and J. M. Ottino, "Surface Flows of Granular Materials: Model and Experiments in Heap Formation," *J. Fluid Mech.*, 441, 255 (2001a).

Khakhar, D. V., J. J. McCarthy, and J. M. Ottino, "Radial Segregation of Granular Mixtures in Rotating Cylinders," *Phys. Fluids*, **9**, 3600 (1997a).

Khakhar, D. V., J. J. McCarthy, J. F. Gilchrist, and J. M. Ottino, "Chaotic Mixing of Granular Materials in 2D Tumbling Mixers," *CHAOS*, **9**, 195 (1999).

Khakhar, D. V., J. J. McCarthy, T. Shinbrot, and J. M. Ottino, "Transverse Flow and Mixing of Granular Materials in a Rotating Cylinder," *Phys. Fluids*, **9**, 31 (1997b).

Khakhar, D. V., A. V. Orpe, and J. M. Ottino, "Surface Granular Flows: Two Related Examples," *Advances in Complex Systems*, **4**, 407 (2001b).

Komatsu, T. S., S. Inagaki, N. Nakagawa, and S. Nasuno, "Creep Motion in a Granular Pile Exhibiting Steady Surface Flow," *Phys. Rev. Lett.*, **86**, 1757 (2001).

Laurent, B. F. C., and J. Bridgwater, "Dispersive Granular Flow in a Horizontal Drum Stirred by a Single Blade," *AIChE J.*, **48**, 50 (2002).

Laurent, B. F. C., J. Bridgwater, and D. J. Parker, "Motion in a Particle Bed Agitated by a Single Bed," *AIChE J.*, **46**, 1723 (2000).

Lun, C. K. K., S. B. Savage, D. J. Jeffrey, and N. Chepurniy, "Kinetic Theories for Granular Flow: Inelastic Particles in Couette Flow and Slightly Inelastic Particles in a General Flow Field," *J. Fluid Mech.*, **140**, 223 (1984).

Makse, H. A., "Continuous Avalanche Segregation of Granular Mixtures in Thin Rotating Drums," *Phys. Rev. Lett.*, **83**, 3186 (1999).

McCarthy, J. J., T. Shinbrot, G. Metcalfe, J. E. Wolf, and J. M. Ottino, "Mixing of Granular Materials in Slowly Rotated Containers," *AIChE J.*, **42**, 3351 (1996).

Nase, S. T., W. L. Vargas, A. A. Abatan, and J. J. McCarthy, "Discrete Characterization Tools for Wet Granular Media," *Powder Technol.*, **116**, 214 (2001).

Orpe, A. V., and D. V. Khakhar, "Scaling Relations for Granular Flow in Quasi-Two-Dimensional Rotating Cylinders," *Phys. Rev. E*, **64**, 031302 (2001).

Ottino, J. M., and D. V. Khakhar, "Fundamental Research in Heaping, Mixing, and Segregation of Granular Materials: Challenges and Perspectives," *Powder Technol.*, **121**, 117 (2001).

Ottino, J. M., and D. V. Khakhar, "Mixing and Segregation of Granular Materials," *Ann. Rev. of Fluid Mech.*, **32**, 55 (2000).

Ottino, J. M., and T. Shinbrot, "Comparing Extremes: Mixing of Fluids, Mixing of Solids," *Mixing: Chaos & Turbulence*, H. Chaté, E. Villermaux, and J.-M. Chomaz, eds., NATO Science Series, Kluwer Academic/Plenum Publishers, New York, pp. 163–186, (1999).

Rajchenbach, J., "Flow in Powders: From Discrete Avalanches to Continuous Regime," *Phys. Rev. Lett.*, **65**, 2221 (1990).

Rao, S. J., S. K. Bhatia, and D. V. Khakhar, "Axial Transport of Granular Solids in Rotating Cylinders. Part 2: Experiments in a Non-Flow System," *Powder Technol.*, **67**, 153 (1991).

Samadani, A., and A. Kudrolli, "Segregation Transitions in Wet Granular Matter," *Phys. Rev. Lett.*, **85**, 5102 (2000).

Savage, S. B., "Disorder, Diffusion and Structure Formation in Granular Flow," *Disorder and Granular Media*, D. Bideau and A. Hansen, eds., Elsevier Science, Amsterdam, pp. 255–285 (1993).

Stewart, R. L., J. Bridgwater, Y. C. Zhou, and A. B. Yu, "Simulated and Measured Flow of Granules in a Bladed Mixer—A Detailed Comparison," *Chem. Eng. Sci.,* **56**, 5457 (2001).

Appendix: Analysis of Spraying of Particles

Consider particles flowing at a constant velocity u being sprayed by a solution at a uniform rate q (mass of coating material per unit area per unit time), as shown in Figure A1. The particles also diffuse in the direction perpendicular to the flow due to interparticle collisions with a diffusivity D_{coll}. For simplicity, consider the flowing layer to be very deep compared to the diffusional distance δ. The variation of the concentration of the coating C (mass of coating per unit volume of particles) is then given by

$$\frac{\partial C}{\partial t} = D_{\text{coll}} \frac{\partial^2 C}{\partial y^2} \tag{A1}$$

where $t = x/u$ is the time of exposure of the particles to the spray. The initial condition and boundary conditions for the problem are

$$C = 0, \quad t = 0 \tag{A2a}$$

$$C = 0, \quad y \to \infty \tag{A2b}$$

$$-D_{\text{coll}} \frac{\partial C}{\partial y} = q, \quad y = 0 \tag{A2c}$$

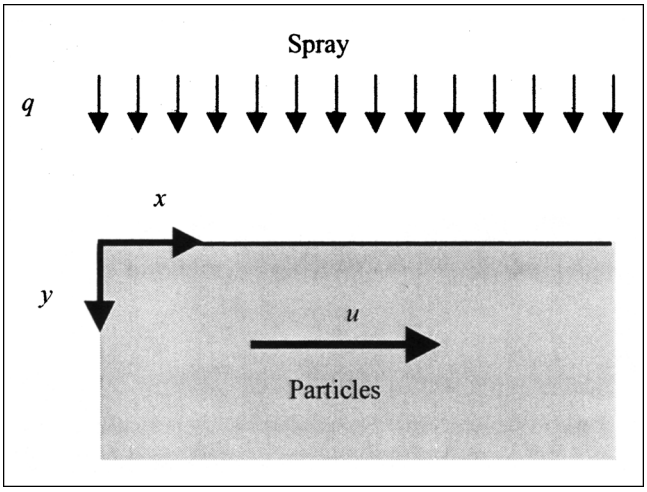

Figure A1. Flowing layer in the spray coating system.

The coordinate system used in the analysis is shown.

The characteristic diffusional length scale from Eq. A1 is $\delta = (D_{coll}t)^{1/2}$, and from Eq. A2c, we get the characteristic concentration at the surface as $C_0 = q\delta/D = q(t/D_{coll})^{1/2}$. Thus, the solution should be of the form $C = C_0 f(\eta)$, where $\eta = y/\delta$. Substituting into the governing equation and applying the boundary conditions, we get the solution to Eq. A1 subject to the initial and boundary conditions given in Eq. A2 as

$$C = q\left(\frac{2t}{D_{coll}}\right)^{1/2}\int_{\eta}^{\infty}\text{erfc}(\eta')d\eta'. \qquad \text{(A3)}$$

Thus, the penetration depth (depth at which the concentration to a small value relative to the surface concentration, say $0.01C_0$) is then the same as in the classical Higbie penetration theory and is given by $(D_{coll}t)^{1/2}$. The above result may be applied to the rotating cylinder case if the shearing motion in the layer is neglected.

Manuscript received Mar. 25, 2002, and revision received June 12, 2002.